

## ADAM17 stabilizes its interacting partner inactive Rhomboid 2 (iRhom2) but not inactive Rhomboid 1 (iRhom1)

Gisela Weskamp<sup>1</sup>, Johanna Tüshaus<sup>2,3,4</sup>, Daniel Li<sup>1</sup>, Regina Feederle<sup>4,5</sup>, Thorsten Maretzky<sup>6</sup>, Steven Swendemann<sup>1</sup>, Erik Falck-Pedersen<sup>7</sup>, David R. McIlwain<sup>8</sup>, Tak W. Mak<sup>9</sup>, Jane E. Salmon<sup>10,11</sup>, Stefan F. Lichtenthaler<sup>2,3,12,13</sup>, Carl P. Blobel<sup>1,2,11,14,\*</sup>

<sup>1</sup>Arthritis and Tissue Degeneration Program, Hospital for Special Surgery, New York, NY 10021, USA, <sup>2</sup>Institute for Advanced Study, Technical University Munich, 85748 Garching, Germany, <sup>3</sup>Neuroproteomics, School of Medicine, Klinikum rechts der Isar, Technical University Munich, 81675 Munich, Germany, <sup>4</sup>German Center for Neurodegenerative Diseases, 81377, Munich, Germany, <sup>5</sup>Institute for Diabetes and Obesity, Monoclonal Antibody Core Facility, Helmholtz Zentrum Munich, German Research Center for Environmental Health, 85764 Neuherberg, Germany, <sup>6</sup>Inflammation Program and Department of Internal Medicine, Roy J. and Lucille A. Carver College of Medicine, University of Iowa, Iowa City, IA, USA, 52242, <sup>7</sup>Dept. of Biochemistry, Cellular and Molecular Biology, Weill Cornell Medicine, New York, NY, 10021, USA, <sup>8</sup>Baxter Laboratory in Stem Cell Biology, Department of Microbiology and Immunology, Stanford University, Stanford, CA, 94305, USA. <sup>9</sup>Campbell Family Institute for Breast Cancer Research, Ontario Cancer Institute, University Health Network, Toronto, M5G 2M9 Ontario, Canada, <sup>10</sup>Autoimmunity and Inflammation Program, Hospital for Special Surgery, New York, NY, 10021, USA, <sup>11</sup>Department of Medicine, Weill Cornell Medicine, New York, NY, 10021, <sup>12</sup>German Center for Neurodegenerative Diseases (DZNE), Munich, Germany, <sup>13</sup>Munich Cluster for Systems Neurology (SyNergy), Munich, Germany, <sup>14</sup>Department of Physiology, Biophysics and Systems Biology, Weill Cornell Medicine, New York, NY, 10021, USA.

Running title: *iRhom2 is stabilized by ADAM17, but iRhom1 is not*

\*Address correspondence to: Dr. Carl P. Blobel, Arthritis and Tissue Degeneration Program, Hospital for Special Surgery at Weill Cornell Medicine, 535 E 70th Street, New York, NY, 10021; phone: 212-606-1429, fax: 212-774-2560, email: [blobelc@hss.edu](mailto:blobelc@hss.edu)

**Keywords:** ADAM17, inactive Rhomboid 1, iRhom1, Rhbdf1, inactive Rhomboid 2, iRhom2, Rhbdf2, stimulator of interferon genes, STING, cell surface enzyme, membrane protein, protein stability, myeloid cell

### Abstract

The metalloprotease ADAM17 (a disintegrin and metalloprotease 17) is a key regulator of tumor necrosis factor  $\alpha$  (TNF $\alpha$ ), interleukin 6 receptor (IL-6R), and epidermal growth factor receptor (EGFR) signaling. ADAM17 maturation and function depend on the seven membrane-spanning inactive rhomboid-like proteins 1 and 2 (iRhom1/2 or Rhbdf1/2). Most studies to date have focused on overexpressed iRhom1 and 2, so only little is known about the

properties of the endogenous proteins. Here, we show that endogenous iRhom1 and 2 can be cell-surface biotinylated on mouse embryonic fibroblasts (mEFs), revealing that endogenous iRhom1 and 2 proteins are present on the cell surface, and that iRhom2 also is present on the surface of lipopolysaccharide (LPS)-stimulated primary bone marrow-derived macrophages (BMDM). Interestingly, very little, if any iRhom2 was detectable in mEFs or BMDMs lacking ADAM17, suggesting that iRhom2 is stabilized by

ADAM17. By contrast, the levels of iRhom1 were slightly increased in the absence of ADAM17 in mEFs, indicating that its stability does not depend on ADAM17. These findings support a model in which iRhom2 and ADAM17 are obligate binding partners and indicate that iRhom2 stability requires the presence of ADAM17, whereas iRhom1 is stable in the absence of ADAM17.

## Introduction

ADAM17 is a cell surface metalloprotease that is required for the proteolytic processing of tumor necrosis factor  $\alpha$  (TNF $\alpha$ ) and is therefore also referred to as TACE (TNF $\alpha$  convertase). In addition, ADAM17 has a crucial role in the proteolytic release and activation of several ligands of the epidermal growth factor receptor (EGFR) as well as of the IL-6-receptor (IL-6R) and other membrane proteins (1-7). Major functions of ADAM17 include the regulation of the EGFR signaling pathway during development (4,8-10) and protection of the skin and intestinal barrier in adults (11-14). Moreover, ADAM17 can contribute to cancers that involve inappropriate EGFR signaling (15,16) and to pathologies involving dysregulated TNF $\alpha$  and IL-6R pathways, including autoimmune diseases such as Rheumatoid Arthritis (17,18).

ADAM17 can be rapidly and post-translationally activated by a number of different signaling pathways (19-23), and requires its transmembrane domain, but not its cytoplasmic domain for this rapid posttranslational activation (19). The seven-membrane spanning protein iRhom2 (inactive Rhomboid 2, also referred to as Rhbdf2, Rhomboid 5 Homolog 2) was identified as a crucial regulator of the maturation of ADAM17 in

bone marrow-derived macrophages (BMDM) (24,25). Additional insight into the relationship of ADAM17 and iRhom2 was provided by a point mutation in the first transmembrane domain (TMD) of iRhom2, termed sinecure, which results in a strong reduction of ADAM17-dependent TNF $\alpha$  release from BMDM (26). Mice that are homozygous for the iRhom2 sinecure mutation and also lack the related iRhom1 resemble previously described *iRhom1/2*<sup>-/-</sup> double knockout mice (27,28), demonstrating that the sinecure point mutation in the first TMD of iRhom2 results in a strongly hypomorphic phenotype. Moreover, the substrate selectivity of ADAM17 is differentially regulated by iRhom1 and 2 (29), and point mutations in the TMD of ADAM17 that were predicted to affect the interaction with iRhom2 strongly reduced iRhom2/ADAM17-dependent shedding events, without affecting iRhom1/ADAM17-dependent shedding (28). The different substrate selectivity of iRhom2/ADAM17 and iRhom1/ADAM17-dependent shedding (29), the effects of the sinecure mutation on ADAM17 and the effects of point mutations in the TMD of ADAM17 on ADAM17/iRhom2-dependent shedding (28) suggested that iRhom2 and ADAM17 form a heteromeric complex. Presumably, this complex associates in the endoplasmic reticulum (ER) and remains together to regulate iRhom2/ADAM17-dependent shedding on the cell surface or in the late secretory pathway. This model is further supported by recent studies demonstrating that mutations in cytoplasmic phosphorylation sites of iRhom2 affect the activation of ADAM17 (30,31). In addition, a newly discovered iRhom2-interacting protein, termed Frmd8 (FERM Domain Containing 8) or iTAP (iRhom tail associated protein), was found to

regulate endocytosis of iRhom2/ADAM17 and degradation in the lysosome (32,33).

Most studies on iRhom1 and 2 to date have focused on the overexpressed proteins (29-34), so there is a paucity of information on the cell biological properties of endogenous iRhom1 and only limited information on iRhom2 (25). The main goal of the current study was to perform a biochemical characterization of endogenous iRhom2 using primary mouse macrophage cultures and mouse embryonic fibroblasts. In light of the crucial role of iRhom2 in regulating the maturation and function of ADAM17 (27) we were also interested in whether ADAM17 reciprocally affects the stability of iRhom2 and the related iRhom1 and their transport to the cell surface. Moreover, since iRhom2 has been shown to interact with the multi-membrane spanning protein stimulator of interferon genes (STING) (35), this raised questions about the role of STING in the stability and maturation of iRhom2 and ADAM17.

## Results

### **Characterization of murine iRhom2 in primary bone marrow-derived macrophages**

In order to characterize endogenous mouse iRhom2, we raised rabbit polyclonal antibodies (pAbs) against a portion of the N-terminal cytoplasmic domain of murine iRhom2 (amino acid residues 1 – 376, see Experimental Procedures for details). These anti-iRhom2 pAbs were tested on lysates of primary bone marrow-derived macrophages (BMDM) isolated from *iRhom2*<sup>-/-</sup> mice or wild type controls. Since the expression of iRhom2 is

upregulated by treatment with LPS (36), we compared untreated BMDM to cells that had been stimulated with 10 ng/ml LPS overnight. LPS treatment induced a band of ~95 kD in wild type BMDM (marked by an asterisk in Figure 1 A, top panel) that was not present in *iRhom2*<sup>-/-</sup> BMDM. However, the anti-iRhom2-pAbs also reacted with several other proteins on blots of the BMDM lysates that were present in *iRhom2*-deficient samples, and thus non-specific (Figure 1 A, top panel). The LPS treatment strongly induced the levels of pro- and mature ADAM17 in wild type BMDM but only of pro-ADAM17 in *iRhom2*<sup>-/-</sup> BMDM (Fig. 1A, middle panel, tubulin served as loading control, lower panel).

To improve detection of the seven-membrane spanning iRhom2 and remove non-specifically recognized soluble proteins, we purified cellular membranes by high-speed centrifugation to enrich for membrane proteins (see Experimental Procedures for details). Western blot analysis of the purified material using the same anti-iRhom2 (1-376) rabbit pAbs revealed a strong band of ~95 kD in the LPS-treated wild type BMDM sample that was not present in the identically prepared *iRhom2*<sup>-/-</sup> control (Figure 1 B, top panel). Moreover, both pro- and mature ADAM17 were present in the whole lysate and membrane preparations from wild type BMDM, whereas only pro-ADAM17 could be detected in the *iRhom2*<sup>-/-</sup> sample, but not mature ADAM17, as previously reported (24,25) (Figure 1 A and B, middle panels, the membrane-anchored ADAM10 (A10) served as a loading control in the lower panel of Figure 1B).

### **Cell surface biotinylation of endogenous iRhom2 in LPS-stimulated BMDM**

To establish whether the endogenous iRhom2 is present on the cell surface of LPS-treated BMDM, a non-membrane permeable biotinylation reagent (Sulfo-NHS-LC-Biotin) was used to label cell surface proteins on these cells (see Experimental Procedures for details). When a Western blot of the purified biotinylated material was probed with anti-iRhom2 pAbs, a band of 95 kD was detected in wild type BMDM, but not in *iRhom2*<sup>-/-</sup> BMDM (Figure 2, top panel). Endoglycosidase H (EndoH) typically cannot process N-linked carbohydrates from glycoproteins that have migrated through the medial Golgi apparatus. However, EndoH treatment of purified cell surface iRhom2 led to slightly faster migration of cell surface biotinylated iRhom2 (Figure 2, top panel). When we instead treated these same samples with PNGase F, which removes all N-linked carbohydrate residues, iRhom2 migrated faster than the EndoH treated sample (Figure 2, top panel). The partial susceptibility of N-linked carbohydrates in cell surface biotinylated iRhom2 to treatment with EndoH was reminiscent of the effect of EndoH and PNGaseF in Western blots of total iRhom2 in BMDM lysates in a prior report (25). The finding that the surface-labeled iRhom2 is partially susceptible to EndoH treatment demonstrates that iRhom2 progresses through the medial Golgi apparatus on the way to the cell surface, and that at least one N-linked carbohydrate residue in iRhom2 does not acquire EndoH resistance (25). Similarly, blots of the cell surface biotinylated ADAM17 in wild type BMDM showed resistance to EndoH (Figure 2 left panel), but sensitivity to PNGaseF, consistent with previous

studies on mature ADAM17 (25,37). These results also corroborated that no mature ADAM17 could be biotinylated on the surface of *iRhom2*<sup>-/-</sup> BMDM (24,25). Finally, cell surface biotinylated ADAM9 was included as a control for the *iRhom2*<sup>-/-</sup> BMDM. Like iRhom2, cell surface labeled ADAM9 is also partially sensitive to EndoH treatment, as previously described (38). To rule out nonspecific binding of iRhom2, ADAM17 or ADAM9 to the streptavidin-sepharose beads used to precipitate cell-surface biotinylated proteins, we incubated extracts of equivalent cultures of wild type cells that were either untreated or cell surface biotinylated with streptavidin beads and performed a Western blot analysis on the bound proteins (Figure 2B). These experiments confirmed that only the biotinylated forms of iRhom2, ADAM17 and ADAM9 bound to streptavidin beads under the conditions used here, whereas these proteins in the lysate of an equivalent number of untreated cells did not. The finding that endogenous iRhom2 can be biotinylated using a non-membrane-permeable biotinylation reagent demonstrates that endogenous iRhom2 is present on the cell surface of primary BMDM, similar to RAW264.7 cells (31).

### **ADAM17 is required for the stabilization of iRhom2**

*iRhom2*-deficient BMDM lack mature ADAM17, whereas the levels of pro-ADAM17 do not appear to be significantly affected (24,25). This raises questions about whether the loss of ADAM17 would reciprocally affect the levels iRhom2. Since *Adam17*<sup>-/-</sup> mice die at birth, we isolated macrophages from the livers of newborn *Adam17*<sup>-/-</sup> mice and their wild type control littermates to assess the fate of iRhom2 in myeloid cells in the absence

of ADAM17. iRhom2 was only weakly detectable in membrane preparations of unstimulated newborn liver derived macrophages (NLDM) from wild type mice (Figure 3 A, top panel, left lane). However, stimulation with 10 ng/ml LPS increased the production of both iRhom2 and ADAM17 in wild type NLDM (Figure 3 A, top and middle panels, right lane), just as in BMDM from adult mice (Figure 1). Interestingly, iRhom2 protein could not be detected by the polyclonal iRhom2 antibody in a Western blot analysis of membrane preparations of LPS-stimulated *Adam17*<sup>-/-</sup> NLDM (Figure 3B, top panel, iRhom2; middle panel, ADAM17, lower panel, ADAM10 control).

To further explore the role of ADAM17 in stabilizing iRhom2 in mouse embryos, isolated membrane preparations from extracts of newborn mice (see Experimental Procedures for details) were probed for iRhom2 or ADAM17. No iRhom2 could be detected in embryos lacking ADAM17 or iRhom2, although both ADAM17 and iRhom2 were present in wild type control extracts (Figure 3 C). Moreover, pro- and mature ADAM17 were present in extracts of newborn *iRhom2*<sup>-/-</sup> mice, where maturation of ADAM17 is supported by iRhom1 (27).

### **Analysis of mRNA expression**

The stabilization of iRhom2 by ADAM17 could depend on the requirement for a continuous interaction of the two heteromeric binding partners, or alternatively, ADAM17 may have a role in controlling the transcription of iRhom2. We therefore performed a qPCR analysis of the expression of iRhom2 in NLDM from wild type, *iRhom2*<sup>-/-</sup>, or *Adam17*<sup>-/-</sup> mice. The results demonstrated that the levels of iRhom2 mRNA were similar in NLDM from wild type and *Adam17*<sup>-/-</sup>

mice, whereas no iRhom2 mRNA was detected in NLDM from *iRhom2*<sup>-/-</sup> mice (Fig. 4 A). These findings argue against a role of ADAM17 in regulating the gene expression of iRhom2. We also addressed whether the catalytic activity of ADAM17 could have a role in regulating the levels of iRhom2, such as by affecting a putative signaling pathway with a role in regulating iRhom2 protein levels. However, when we incubated wild type BMDM with the general metalloproteinase inhibitor marimastat (MM), there was no significant effect on the levels of iRhom2 protein (Figure 4 B).

### **Effect of protein degradation inhibitors on iRhom2 stability**

We next considered possible degradation pathways for iRhom2 in the absence of ADAM17. We therefore incubated LPS-stimulated BMDM from mice, in which floxed alleles of ADAM17 were conditionally inactivated in myeloid cells through expression of *LysM-Cre* (*A17LysM-Cre* mice) with an inhibitor of proteasomal degradation (MG132, 10 $\mu$ M) (30,39), an inhibitor of ER associated degradation (Eeyarestatin, 10 $\mu$ M) (40) and inhibitors of lysosomal acidification and autophagosome-lysosome fusion (Chloroquine, 100 $\mu$ M, Bafilomycin, 100nM) (41,42). However, at these concentrations, which have been reported to be effective in cell-based assays (see Experimental Procedures for details) neither of these degradation inhibitors had a significant effect on enhancing the stability of iRhom2, as detected by Western blot (Fig. 5 A, ADAM10 shown as loading control). Similar results were obtained when these inhibitors were tested on *A17*<sup>-/-</sup> mEFs (Figure 5 B). In a control experiment for the activity of the degradation inhibitors in wild type mEFs,

we found that 10 $\mu$ M Eeyarestatin or 10  $\mu$ M MG132 effectively inhibited ubiquitin degradation (Figure 5C) (43). Moreover, addition of 100nM Bafilomycin or 100 $\mu$ M Chloroquine led to a strong increase in LC3-II, an accepted marker of autophagy inhibition (44) (Figure 5 D), corroborating the activity of these compounds.

### ***STING is not required for the stability of iRhom2***

The multi-membrane spanning protein stimulator of interferon genes (STING) has been reported as an interacting partner of iRhom2 (35). In order to determine whether STING is required to stabilize iRhom2, we isolated BMDM from *Sting*<sup>-/-</sup> mice, from wild type controls. As shown in figure 6 A, the lack of STING had no detectable effect on the protein levels of iRhom2 or ADAM17. Moreover, we found that inactivation of iRhom2 in BMDM also did not have a strong effect on the levels of STING that were detectable by Western blot analysis (Figure 6 B). Finally, the mRNA levels for iRhom2 were comparable in BMDM from WT and *Sting*<sup>-/-</sup> mice, but undetectable in BMDM from *iRhom2*<sup>-/-</sup> mice (Figure 6 C).

### ***Analysis of the levels of iRhom2 and the related iRhom1 in mEFs lacking ADAM17***

When we attempted to detect the endogenous iRhom2 in Western blots of mouse embryonic fibroblasts, we found that the rabbit anti-iRhom2 (1-376) polyclonal antibodies against the cytoplasmic domain of iRhom2 were not reproducibly effective for this purpose (data not shown). Therefore, new rat monoclonal antibodies (mAbs) against mouse iRhom1 or iRhom2 were generated (see Experimental Procedures for details). As shown in

Figure 7 A, the rat mAbs specifically recognized iRhom1 or 2 in WT mEFs, with mEFs lacking iRhom1 (iR1KO) or iRhom2 (iR2KO) or both iRhom1 and 2 (iR1/2DKO) serving as controls for the specificity of these mAbs. We noted that the levels of iRhom2 were not significantly affected by the absence of iRhom1 and that the anti-iRhom2 rat mAb recognized a small, but detectable amount of iRhom2 in *A17*<sup>-/-</sup> mEFs. The rat mAb against iRhom1 demonstrated that the levels of iRhom1 were not significantly changed in *iRhom2*<sup>-/-</sup> mEFs, but they appeared slightly increased in the *A17*<sup>-/-</sup> mEFs. Cell surface biotinylation of WT mEFs showed that both iRhom1 and iRhom2 could be detected on the cell surface of these cells (Figure 7 B). The cell surface biotinylation of only the mature form of ADAM17 and of ADAM9, used as loading control, but not their pro-forms served as an internal control that the biotinylation reagent was specific for cell surface proteins and did not label intracellular proteins, in this case pro-ADAM17 or pro-ADAM9.

### **Discussion**

Previous studies have shown that pro-ADAM17 is synthesized in the absence of iRhom2 in BMDM, but not transported out of the ER to the trans Golgi network (TGN), where its pro-domain is removed (24,45). This finding raised questions about the fate of iRhom2 in the absence of ADAM17, or in the absence of a recently identified iRhom2-binding partner, STING. Moreover, since mEFs lacking both iRhom1 and iRhom2 only have pro-ADAM17, but no detectable mature ADAM17, we were interested in exploring whether endogenous iRhom2 and the related iRhom1 can be detected

on the cell surface of wild type mEFs, as would be predicted if they can function as regulators of endogenous mature ADAM17. Finally, we were interested in whether the lack of ADAM17 reciprocally affects the stability of iRhom1 and 2.

Our observation that little, if any iRhom2 is detectable by Western blot in myeloid cells or in embryos lacking ADAM17 under conditions where it can readily be detected in wild-type controls, provides the first evidence that ADAM17 is required for the stabilization of endogenous iRhom2. Unlike pro-ADAM17, which is present at comparable levels in wild type and *iRhom2*<sup>-/-</sup> BMDM and can be upregulated by treatment of BMDM with LPS, we found no detectable iRhom2 in membrane preparations of LPS-treated *Adam17*<sup>-/-</sup> NLDM. Treatment with inhibitors of proteasomal degradation, ER-associated degradation or lysosomal acidification and degradation did not restore the ability to detect iRhom2 in *Adam17*<sup>-/-</sup> NLDM or in *Adam17*<sup>-/-</sup> mEFs, arguing against a major role of these pathways in controlling the stability of iRhom2 in the absence of ADAM17. In addition, we found that the lack of ADAM17 did not affect mRNA levels of iRhom2 in LPS-treated NLDM. Finally, the catalytic activity of ADAM17 is most likely not required for the stabilization of iRhom2, since the general metalloprotease inhibitor marimastat had no detectable effects on the levels of iRhom2. Further studies will be necessary to better understand the mechanism of how the stability of iRhom2 is regulated in the absence of ADAM17. Taken together, these results suggest that the presence of the ADAM17 is required for the stabilization of iRhom2. Conversely, since only the mature form of ADAM17 is

affected by the lack of iRhom2 in BMDM (24,25) or NLDM, whereas the pro-form is not, these results suggest that pro-ADAM17 is produced at similar levels in the presence or absence of iRhom2, and does not require iRhom2 for stabilization.

The observation that pro-ADAM17 can exist in the absence of iRhom2, but requires iRhom2 to be converted into its mature, processed and EndoH-resistant form, supports a model in which pro-ADAM17 assembles with newly synthesized iRhom2 in the endoplasmic reticulum (ER), allowing both to exit the ER and enter the secretory pathway together. The pro-domain of ADAM17 is then removed by pro-protein convertases in the trans-Golgi network (37,46). This is a pre-requisite for the activity of ADAM17, which can be rapidly enhanced by many different stimuli once ADAM17 has been processed by pro-protein convertases (19,46). The inability to detect iRhom2 in the absence of ADAM17 in NLDM and in embryos and the very low levels of iRhom2 in *A17*<sup>-/-</sup> mEFs suggests that it is unstable without its binding partner. Moreover, since pro-ADAM17 is stable in the absence of iRhom2, this suggests that iRhom2 can associate with pre-existing molecules of ADAM17 to form an iRhom2/ADAM17 complex, presumably after pro-ADAM17 has been translocated across the ER membrane.

iRhom2 also interacts with another multi-membrane spanning protein, STING, which is involved in regulating innate immunity to DNA viruses (35). However, we found that STING is not essential for the stabilization of the iRhom2/ADAM17 complex. In addition, iRhom2 also interacts with several cytoplasmic molecules, including members of the 14-

3-3 family of signaling adapters and FRMD8/iTAP (30-33). Moreover, since iRhom2 determines the substrate selectivity of ADAM17, the iRhom2/ADAM17 complex most likely also interacts with its substrates. This notion is further supported by the observation that the phenotype caused by the “curly-bare” (cub) mutation in the cytoplasmic domain of iRhom2 (curly hair and bare skin) is only seen in the presence of the iRhom2/ADAM17 substrate amphiregulin, but not in mice lacking amphiregulin (47,48). Presumably, the interaction between wild type iRhom2/ADAM17 and its substrates is transient, so as to allow rapid substrate turnover upon activation of ADAM17.

Similar to iRhom2, the related iRhom1 can be detected on the surface of mouse embryonic fibroblasts. However, unlike iRhom2, the levels of iRhom1 are not significantly affected in the absence of ADAM17, suggesting that it interacts differently with ADAM17 than iRhom2 and can be stable on its own. The migration of the biotinylated iRhom1 or iRhom2 was comparable to that of their non-biotinylated counterparts that could be detected by Western in whole lysates, suggesting that the iRhom1 and 2 proteins do not undergo substantial proteolytic processing en route through the secretory pathway to the cell surface. It will be interesting to characterize the interaction between iRhom1 and ADAM17 in more detail in the future.

In summary, our results provide the first evidence that endogenous iRhom2 is stabilized by the presence of ADAM17, whereas iRhom1 is not. Nevertheless, both iRhom proteins can be detected on the cell surface of wild type cells, where they presumably interact with ADAM17.

Interestingly, a second interacting partner of iRhom2, the stimulator of interferon genes (STING) is not required for the stability of iRhom2. These findings support a model, in which ADAM17 is a principal partner or client of iRhom2, and in which both must be present to support the maturation and function of the iRhom2/ADAM17 complex on the cell surface.

## **Experimental Procedures:**

### ***Reagents and antibodies***

All reagents were purchased from Sigma/Aldrich, St. Louis, MO, unless specified otherwise. The rabbit antibodies against the cytoplasmic domain of iRhom2 were generated by immunizing female New Zealand White rabbits with a gst-fusion protein with the cytoplasmic domain of mouse iRhom2 (amino acid residues 1-376, ProSci Inc., Poway, CA). The rat anti-iRhom1 and anti-iRhom2 monoclonal antibodies were generated using standard procedures (49). The iRhom1 antibody (RHF1A 20A8; IgG2a) was generated by immunization of ovalbumin-coupled peptide MSEARRDSTSSLQRKKPPW. For the anti-iRhom2 antibody (RHF2B 11H7; IgG2a) ovalbumin-coupled peptide GDWEGKRQNWHRSL was used. Antibodies against the cytoplasmic domain of mouse ADAM9 and ADAM17 have been previously described (37,50). Antibodies against A10 were from AbCam, Cambridge, MA (Cat#1244695), antibodies against STING and antibodies against mouse tubulin were from Cell Signaling, Danvers, MA; antibodies against GAPDH were from ABclonal, Woburn, MA. Anti-LC3 was from Novus Biological, Littleton, CO (Cat # Nb100-2220), and anti-Ubiquitin Clone P4G7 was from Biologend, San Diego, CA

(Cat# 838703). The deglycosylation enzymes endoglycosidase H (EndoH) and protein-N-glycanase F (PNGase F) were from NEB, Ipswich, MA. EZ-Link Sulfo-NHS-LC-Biotin was from Thermo Fisher Scientific, Waltham, MA (Cat. # 21335). Streptavidin-Sepharose 4B beads were from Thermo Fisher (Cat#434341). Sigma Aldrich, St. Louis, MO was the source for Chloroquine (Cat#C6628), MG132 (Cat#474790), Bafilomycin (Cat# B1793) and Eeyarestatin (Cat# E1286). The inhibitors of protein degradation or endocytosis were used at following concentration and for the times indicated: MG132 at 10 $\mu$ M for 18h (33); Chloroquine at 100 $\mu$ M for 18h (33); Bafilomycin at 100nM for 18h (32) and Eeyarestatin at 10 $\mu$ M for 18h (43). Marimastat was a gift from Dr. Ouathék Ouerfelli, Memorial Sloan-Kettering Cancer Center, New York, NY (51).

### **Mouse lines**

*iRhom2*<sup>-/-</sup> mice and *Adam17*<sup>-/-</sup> mice have been described previously (5,24). *Sting*<sup>-/-</sup> mice were kindly provided by Dr. Liang Deng, MSKCC (52,53). All animal experiments were approved by the Institutional Animal Use and Care Committee of the Hospital for Special Surgery and Weill Cornell Medicine.

### **Isolation and generation of mouse primary macrophages**

In order to generate primary bone marrow-derived macrophages (BMDM), we harvested and cultured the bone marrow cells of 4 week-old mice (equal distribution of male and female mice) as previously described (17). Briefly, femurs and tibiae were flushed with Hank's Balanced Salt Solution (HBSS) and washed cells were plated on petri dishes in RPMI medium supplemented

with 20% fetal calf serum (FCS) and murine macrophage colony stimulating factor (M-CSF, Peprotech, Rocky Hill, NJ) at 10 ng/ml. After 7 days, macrophages were collected with a plastic tissue culture scraper, plated on fresh plates at 1x10<sup>6</sup> cells/10 cm<sup>2</sup> and stimulated with 10 ng/ml LPS for 14-18 hrs. For the preparation of newborn liver-derived macrophages (NLDM) from mice at postnatal day 1 (P1), livers were removed after euthanasia and then dispersed through a 70  $\mu$ m cell strainer (Denville Scientific, Holliston, MA). Red blood cells were removed with red blood cell lysis buffer (Sigma/Aldrich, St. Louis, MO) according to the manufacturer's protocol and cells were then cultured as described above. After 5 days in culture, 2 x 10<sup>6</sup> differentiated NLDM were stimulated with 10ng/ml LPS for 14 hrs and processed for Western blot analysis.

### **Culture of mouse embryonic fibroblasts**

Generation and culture of immortalized mouse embryonic fibroblasts used in this study has been described previously (5,27,29,54).

### **Membrane preparations and lectin purification**

For the preparation of membrane protein extracts from BMDM or NLDM, cells were washed twice with PBS and then scraped directly in membrane buffer (250 mM Sucrose, 20 mM Hepes, pH 7.4, 10 mM KCl, 1.5 mM MgCl<sub>2</sub>, 1mM EGTA, 1mM EDTA) containing protease inhibitors plus 5 mM of the zinc-binding chelator 1,10 Phenanthroline (24,37). For membrane preparations from newborn mice (P1), the animals were euthanized, and the remaining tissues were minced with razor blades and then mechanically dispersed and subjected to two 30

second treatments with a Polytron homogenizer (Kinematica, Switzerland) in membrane buffer. The cell suspension or the homogenized tissues were then treated with 30 homogenization cycles in a Dounce Homogenizer (Potter-Elvehjem, Sigma/Aldrich, St. Louis, MA). The cell or tissue suspension was subjected to a low speed spin at 720 x g for 10 min at 4<sup>o</sup> C. The supernatant was subsequently transferred to a 13 ml ultracentrifuge tube (Ultra-Clear tubes, Beckman Coulter; Brea, CA) adjusted to 12.5 ml with membrane buffer and centrifuged for 1 hr at 100,000 x g in a Beckmann Optima X Ultracentrifuge in an SW40 rotor. The resulting membrane pellets were re-suspended by boiling for 5 min. in 1x SDS-sample loading buffer, separated on SDS-polyacrylamide gels, transferred to nitrocellulose membranes (see below) and then probed with antibodies against ADAM10, ADAM17 or iRhom2.

#### **Controls for inhibitors of protein degradation.**

The patterns of ubiquitinated proteins and of a protein affected by autophagy (LC3 II) were evaluated using Western blot analysis. Cells from a 6 well culture dish (Nunc, Thermo Fisher Scientific, Waltham, MA) were incubated with inhibitors for 18 hrs, then washed in PBS and suspended in 1x SDS containing sample loading buffer. The resulting whole cell extracts were sonicated with a Bioruptor Pico sonicator (Diagenode, Denville, NJ) for 3 rounds of 10 sec bursts at maximal strength, then boiled for 5 min and then separated on 10% Bis-Tris NuPage Gels (Thermo Fisher Scientific, Waltham, MA, Cat# NP0301) in MES (2-(N-morpholino)ethane sulfonic acid) buffer according to the manufacturer's instructions. Western

blots were performed as described, with anti-LC3- and anti-Ubiquitin primary antibodies used at 1:1000.

#### **Western Blot analysis.**

To generate Western blots for iRhom2 and ADAM17 from BMDM samples from *iRhom2*<sup>-/-</sup> mice and wild type controls (Figure 1 A) extracts from 1 x 10<sup>6</sup> cells were separated on 10% SDS-PAGE gels and transferred to nitrocellulose membranes (Pall Corp. Port Washington, NY). The Western blots in figures 1 B and Figure 3 A, B, C were performed using extracts from 100,000 x g membrane preparations (see above). Western blots of lysates of mouse embryonic fibroblasts from wild type (WT), *iRhom1*<sup>-/-</sup>, *iRhom2*<sup>-/-</sup>, *iRhom1/2*<sup>-/-</sup> double knockout or *A17*<sup>-/-</sup> knockout E14.5 embryos were performed as described previously (27). After blocking in 5% nonfat milk at room temperature for 1 hour, the nitrocellulose membranes were incubated in primary antibody overnight at 4<sup>o</sup> C (1:2000 dilution for rabbit-anti-iRhom2-cyto), or for 1h at RT (rat monoclonal anti-iRhom1 and anti-iRhom2 antibodies at 1:10 culture supernatant dilution). Sting antibodies (Cell Signaling, Danvers, MA) were each incubated overnight at 4<sup>o</sup> C at 1:1000 dilution. The nitrocellulose membranes were then washed three times in PBS, 0.05% Tween-20 and then incubated in either HRP-labeled goat anti-rabbit secondary antibody, HRP-labeled goat anti-mouse secondary antibody (1:5000, Promega, Madison, WI) or HRP-labeled goat anti-rat secondary antibody (1:5000, Sigma). Bound antibodies were detected using the ECL system (Thermo Fisher Scientific, Waltham, MA) and a Chemdoc image analyzer (Bio-Rad, Hercules, CA), and the images were assembled using Microsoft Powerpoint software. Loading

controls were generated either by Western blotting parallel samples or by stripping membranes for 15 min at 55°C in stripping buffer (2% SDS, 50mM 2-mercaptoethanol in 62mM Tris, pH 6.7). These membranes were blocked as described and then incubated with anti-ADAM9, anti-ADAM10, anti-GAPDH or anti-tubulin antibodies at 1:2000 and the bound antibodies were detected as described above.

### **Cell Surface Biotinylation**

Mouse embryonic fibroblasts or differentiated BMDM that had been left untreated, or had been treated with 10 ng/ml LPS were cell surface biotinylated by incubation with a 1 mg/ml solution of the nonmembrane-permeable biotinylation reagent EZ-Link Sulfo-NHS-LC-Biotin (Thermo Fisher Scientific, Waltham, MA) in sterile PBS for 45 min at 4° C. The reaction was quenched with 0.1 M glycine in PBS and then the cells were lysed in cell lysis buffer (PBS, 1% Triton X-100 containing protease inhibitors plus 5 mM of the zinc-binding chelator 1,10 Phenanthroline (24,37) and 5µM Marimastat). Extracts containing biotinylated proteins were incubated with 10ul washed Streptavidin-Sepharose 4B beads for 30 min at 4°C. The beads were then washed 4 x with cell lysis buffer and bound proteins were eluted in boiling SDS-sample buffer and separated on

NuPAGE Novex 3-8% Tris-Acetate protein gels (Thermo Fisher Scientific, Waltham, MA) and then subjected to Western blot analysis with antibodies against iRhom1 or 2, ADAM17 or ADAM9, as indicated. All other samples were separated on 10% SDS-PAGE gels.

### **RT-qPCR analysis**

Total RNA from cultured wild type, *Adam17*<sup>-/-</sup> or *iRhom2*<sup>-/-</sup> NLDM or from wild type, *iRhom2*<sup>-/-</sup> or *Sting*<sup>-/-</sup> BMDM was isolated with RNeasy (Qiagen, Germantown, MA) and subsequently reverse transcribed (Oligo-dT/SuperScript RT III, Qiagen, Germantown, MA). Oligonucleotides for iR2 and GAPDH were purchased from Qiagen. Sequences for β-actin oligonucleotides were: β-actin forward: 5'-AGGTGTGCACTTTTATTGGTCTCAA-3'; β-actin reverse: 5'-TGTATGAAGGcTTTGGTCTCCCT-3'. RT-qPCR was performed using SYBR Green on an ABI PRISM 7900HT cycler (both Applied Biosystems, Thermo Fisher Scientific, Waltham, MA). GAPDH was used as endogenous control to normalize each sample. Three independent experiments were performed in triplicate.

### **Acknowledgements.**

We thank Elin Mogollon, Sarah Loh and Katrin Moschke for technical assistance, Gregory Farber for help with the RT-qPCR analysis, and NIH R01 GM64750 and R35 GM134907 to CPB for support. The content is solely the responsibility of the authors and does not necessarily represent the official views of the National Institutes of Health. This work was also supported by the Deutsche Forschungsgemeinschaft (German Research Foundation) within the framework of the Munich Cluster for Systems Neurology (EXC 2145 SyNergy, project ID 390857198).

**Conflict of interest**

Drs. McIlwain, Mak, Maretzky and Blobel hold a patent on a method of identifying agents for combination with inhibitors of iRhoms. Dr. Blobel and the Hospital for Special Surgery have identified iRhom2 inhibitors and have co-founded the start-up company SciRhom in Munich to commercialize these inhibitors.

**Authorship contributions**

GW and CPB conceived the study; GW, TM, DL, SS, SFL, JT and EFP designed and performed experiments; TWM provided reagents related to iRhom2; RF in collaboration with SFL generated the rat monoclonal antibodies against iRhom1 and iRhom2, SS generated the rabbit polyclonal antibodies against the cytoplasmic domain of iRhom2, GW, TM, SFL, JT, EFP and DM analyzed data; GW and CPB wrote the manuscript; JT, TM, DM, EFP, JS, RF and SFL made manuscript revisions.

## Figure Legends

**Figure 1. Western Blot analysis of mouse iRhom2 in cell lysates and purified membranes isolated from mouse BMDM.** A) Primary BMDM isolated from wild type (WT) or *iRhom2*<sup>-/-</sup> mice were either not treated or incubated with 10 ng/ml LPS for 14-18 h and then lysed and subjected to Western blot analysis. B) Western blot of high-speed membrane preparations from LPS-treated WT or *iRhom2*<sup>-/-</sup> BMDM showed a strong enrichment of iRhom2 and much weaker non-specific bands compared to the whole cell lysate. The samples were either probed with rabbit polyclonal antibodies against the cytoplasmic domain of mouse iRhom2 (top panels), or antibodies against the cytoplasmic domain of ADAM17 (middle panels), or tubulin or ADAM10, as indicated (lower panels). The bold line in A), middle panel, indicates splicing of non-adjacent lanes. Each figure is representative for 3 separate experiments.

**Figure 2. Labeling of endogenous iRhom2 on the cell surface of primary LPS-stimulated mouse BMDM.** A) LPS-stimulated wild type (WT) or *iRhom2*<sup>-/-</sup> BMDM were incubated with the non-membrane-permeable biotinylation reagent EZ-Link Sulfo-NHS-LC-Biotin. Western blots of biotinylated material isolated with Streptavidin Sepharose 4B beads were either not treated (left lane) or incubated with EndoH (middle lane) or PNGaseF (right lane) and then probed with antibodies against the cytoplasmic domain of iRhom2, ADAM17 (A17) or ADAM9 (A9), as indicated. Panel B) shows a control for the possible non-specific binding of iRhom2, ADAM17 or ADAM9 to Streptavidin Sepharose 4B beads. Two confluent plates each of wild type or *iRhom2*<sup>-/-</sup> BMDM were prepared, and one was subjected to cell surface biotinylation as in panel A, whereas the other was left untreated. Following lysis in cell lysis buffer, both lysates were incubated in streptavidin beads under the same conditions as the samples in panel A. The Western blots are representative for 3 separate experiments with essentially identical results.

**Figure 3. ADAM17 is required for the stabilization of iRhom2 in newborn mouse liver-derived macrophages and in newborn mice.** A) Western blot of a membrane preparation of newborn mouse liver-derived macrophages (NLDM) demonstrates that LPS treatment enhances the production of iRhom2 and ADAM17. B) iRhom2 and ADAM17 can be detected in Western blots of LPS-stimulated wild type (WT), but not in *Adam17*<sup>-/-</sup> NLDM membrane preparations. C) Western blot analysis of membranes prepared from newborn WT mice show iRhom2 and pro- and mature ADAM17, whereas no iRhom2 or ADAM17 can be detected in identically prepared membranes from newborn *Adam17*<sup>-/-</sup> mice. A Western blot of membranes from *iRhom2*<sup>-/-</sup> mice shows no iRhom2, but pro- and mature ADAM17 are present. In each panel, ADAM10 serves as a loading control. Each panel is representative of 3 separate experiments.

**Figure 4. Expression analysis of iRhom2 by RT-qPCR and effect of treatment of wild type cells with the metalloprotease inhibitor marimastat.**

A) An RT-qPCR analysis shows comparable expression of iRhom2 mRNA in wildtype (WT) and *Adam17*<sup>-/-</sup> BMDM (A17<sup>-/-</sup>), but not in *iRhom2*<sup>-/-</sup> BMDM (*iR2*<sup>-/-</sup>), used here as a control. B) LPS stimulated BMDM from WT mice were treated with or without 5µM Marimastat for 18h and then lysed and the samples subjected to Western blot analysis

for iRhom2 or ADAM17, with ADAM10 as a loading control. The bold line in the top panel (iR2 samples) indicates that these two lanes were spliced together. Each experiment was repeated 3 times with essentially similar outcomes, one representative sample is shown.

**Figure 5. Effect of inhibitors of endocytosis or protein degradation on iRhom2 levels in ADAM17-deficient cells.** A) BMDM from *Adam17-LysM-cre* mice or B) *Adam17*<sup>-/-</sup> mEFs were either left untreated or were treated with 10 $\mu$ M MG132, 100 $\mu$ M Chloroquine, 100nM Bafilomycin or 10 $\mu$ M Eeyarastatin I, as indicated, for 18 hours and then subjected to Western blot analysis for iRhom2, ADAM17 or ADAM10 and compared with untreated wild type BMDM (A) or mEFs (B). As controls for the efficacy of the inhibitors, wild type mEFs were incubated under identical conditions as the ADAM17-deficient BMDM (A) or mEFs (B). Whole cell lysates of the wild type mEFs treated with Eeyarastatin I or MG132 were subjected to Western blot analysis with antibodies against Ubiquitin (C), and Western blot of extracts from wild type mEFs treated with Bafilomycin or Chloroquine were probed for LC3-II, a marker for inhibition of autophagy (D). The data are representative of 3 replicates with essentially similar results.

**Figure 6. Expression of Sting, iRhom2 and ADAM17 in BMDM lacking Sting or iRhom2.** Western blot analysis for iRhom2, ADAM17, Sting or ADAM10 was performed on unstimulated or LPS-stimulated BMDM from *Sting*<sup>-/-</sup> mice or wild type (WT) controls (A) or from *iRhom2*<sup>-/-</sup> mice and WT controls (B). The bold line in (B) indicates splicing of non-adjacent lanes. (C) An RT-qPCR analysis was used to confirm that the mRNA for *iRhom2* was expressed at similar levels in *Sting*<sup>-/-</sup> BMDM compared to WT controls. Each experiment was repeated 3 times and representative samples are shown.

**Figure 7. Rat monoclonal antibodies against iRhom1 or 2 allow detection of the endogenous proteins in mEFs.** A) Western blot analysis of extracts of WT mEFs or mEFs lacking *iRhom1* (iR1KO) or *iRhom2* (iR2KO) or *Adam17* (A17KO) or both *iRhom1* and 2 (iR1/2DKO) with rat polyclonal antibodies against iRhom1 or iRhom2 or ADAM17, with GAPDH serving as loading control. B) Western blot analysis of extracts from non-biotinylated WT or iR1/2DKO mEFs (left two lanes) or Streptavidin Sepharose 4B precipitated samples from cell surface biotinylated WT or iR1/2DKO mEFs were probed with antibodies against iRhom1, iRhom2, ADAM17 or ADAM9, which served as a loading control. The bold lines in the top panel of A) and the bottom panel of B) indicate that these lanes were spliced together. These results are representative examples of 3 separate experiments.

## References

1. Blobel, C. P. (2005) ADAMs: key players in EGFR-signaling, development and disease. *Nat. Rev. Mol. Cell. Bio.* **6**, 32-43
2. Weber, S., and Saftig, P. (2012) Ectodomain shedding and ADAMs in development. *Development* **139**, 3693-3709
3. Scheller, J., Chalaris, A., Garbers, C., and Rose-John, S. (2011) ADAM17: a molecular switch to control inflammation and tissue regeneration. *Trends Immunol* **32**, 380-387

4. Peschon, J. J., Slack, J. L., Reddy, P., Stocking, K. L., Sunnarborg, S. W., Lee, D. C., Russel, W. E., Castner, B. J., Johnson, R. S., Fitzner, J. N., Boyce, R. W., Nelson, N., Kozlosky, C. J., Wolfson, M. F., Rauch, C. T., Cerretti, D. P., Paxton, R. J., March, C. J., and Black, R. A. (1998) An essential role for ectodomain shedding in mammalian development. *Science* **282**, 1281-1284
5. Horiuchi, K., Kimura, T., Miyamoto, T., Takaishi, H., Okada, Y., Toyama, Y., and Blobel, C. P. (2007) Cutting Edge: TNF- $\alpha$ -Converting Enzyme (TACE/ADAM17) Inactivation in Mouse Myeloid Cells Prevents Lethality from Endotoxin Shock. *J Immunol* **179**, 2686-2689
6. Black, R., Rauch, C. T., Kozlosky, C. J., Peschon, J. J., Slack, J. L., Wolfson, M. F., Castner, B. J., Stocking, K. L., Reddy, P., Srinivasan, S., Nelson, N., Boiani, N., Schooley, K. A., Gerhart, M., Davis, R., Fitzner, J. N., Johnson, R. S., Paxton, R. J., March, C. J., and Cerretti, D. P. (1997) A metalloprotease disintegrin that releases tumour-necrosis factor- $\alpha$  from cells. *Nature* **385**, 729-733
7. Moss, M. L., Jin, S.-L. C., Milla, M. E., Burkhart, W., Cartner, H. L., Chen, W.-J., Clay, W. C., Didsbury, J. R., Hassler, D., Hoffman, C. R., Kost, T. A., Lambert, M. H., Lessnitzer, M. A., McCauley, P., McGeehan, G., Mitchell, J., Moyer, M., Pahel, G., Rocque, W., Overton, L. K., Schoenen, F., Seaton, T., Su, J.-L., Warner, J., Willard, D., and Becherer, J. D. (1997) Cloning of a disintegrin metalloproteinase that processes precursor tumour-necrosis factor- $\alpha$ . *Nature* **385**, 733-736
8. Jackson, L. F., Qiu, T. H., Sunnarborg, S. W., Chang, A., Zhang, C., Patterson, C., and Lee, D. C. (2003) Defective valvulogenesis in HB-EGF and TACE-null mice is associated with aberrant BMP signaling. *Embo J.* **22**, 2704-2716
9. Sternlicht, M. D., Sunnarborg, S. W., Kouros-Mehr, H., Yu, Y., Lee, D. C., and Werb, Z. (2005) Mammary ductal morphogenesis requires paracrine activation of stromal EGFR via ADAM17-dependent shedding of epithelial amphiregulin. *Development* **132**, 3923-3933
10. Sahin, U., Weskamp, G., Zhou, H. M., Higashiyama, S., Peschon, J. J., Hartmann, D., Saftig, P., and Blobel, C. P. (2004) Distinct roles for ADAM10 and ADAM17 in ectodomain shedding of six EGFR-ligands. *J. Cell Biol.* **164**, 769-779
11. Franzke, C. W., Cobzaru, C., Triantafyllopoulou, A., Loffek, S., Horiuchi, K., Threadgill, D. W., Kurz, T., van Rooijen, N., Bruckner-Tuderman, L., and Blobel, C. P. (2012) Epidermal ADAM17 maintains the skin barrier by regulating EGFR ligand-dependent terminal keratinocyte differentiation. *J Exp Med* **209**, 1105-1119
12. Chalaris, A., Adam, N., Sina, C., Rosenstiel, P., Lehmann-Koch, J., Schirmacher, P., Hartmann, D., Cichy, J., Gavrilo, O., Schreiber, S., Jostock, T., Matthews, V., Hasler, R., Becker, C., Neurath, M. F., Reiss, K., Saftig, P., Scheller, J., and Rose-John, S. (2010) Critical role of the disintegrin metalloprotease ADAM17 for intestinal inflammation and regeneration in mice. *J Exp Med* **207**, 1617-1624
13. Blaydon, D. C., Biancheri, P., Di, W. L., Plagnol, V., Cabral, R. M., Brooke, M. A., van Heel, D. A., Ruschendorf, F., Toynbee, M., Walne, A., O'Toole, E. A., Martin, J. E., Lindley, K., Vulliamy, T., Abrams, D. J., MacDonald, T. T., Harper, J. I., and Kelsell, D. P. (2011) Inflammatory skin and bowel disease linked to ADAM17 deletion. *N Engl J Med* **365**, 1502-1508
14. Tholen, S., Wolf, C., Mayer, B., Knopf, J. D., Loffek, S., Qian, Y., Kizhakkedathu, J. N., Biniossek, M. L., Franzke, C. W., and Schilling, O. (2016) Skin Barrier Defects

- Caused by Keratinocyte-Specific Deletion of ADAM17 or EGFR Are Based on Highly Similar Proteome and Degradome Alterations. *J Proteome Res* **15**, 1402-1417
15. Rossello, A., Nuti, E., Ferrini, S., and Fabbi, M. (2016) Targeting ADAM17 Sheddase Activity in Cancer. *Curr Drug Targets* **17**, 1908-1927
  16. Ardito, C. M., Gruner, B. M., Takeuchi, K. K., Lubeseder-Martellato, C., Teichmann, N., Mazur, P. K., Delgiorno, K. E., Carpenter, E. S., Halbrook, C. J., Hall, J. C., Pal, D., Briel, T., Herner, A., Trajkovic-Arsic, M., Sipos, B., Liou, G. Y., Storz, P., Murray, N. R., Threadgill, D. W., Sibilina, M., Washington, M. K., Wilson, C. L., Schmid, R. M., Raines, E. W., Crawford, H. C., and Siveke, J. T. (2012) EGF receptor is required for KRAS-induced pancreatic tumorigenesis. *Cancer Cell* **22**, 304-317
  17. Issuree, P. D., Maretzky, T., Mcllwain, D. R., Monette, S., Qing, X., Lang, P. A., Swendeman, S. L., Park-Min, K. H., Binder, N., Kalliolias, G. D., Yarilina, A., Horiuchi, K., Ivashkiv, L. B., Mak, T. W., Salmon, J. E., and Blobel, C. P. (2013) iRHOM2 is a critical pathogenic mediator of inflammatory arthritis. *J Clin Invest* **123**, 928-932
  18. Scheller, J., Garbers, C., and Rose-John, S. (2014) Interleukin-6: from basic biology to selective blockade of pro-inflammatory activities. *Semin Immunol* **26**, 2-12
  19. Le Gall, S. M., Maretzky, T., Issuree, P. D. A., Niu, X.-D., Reiss, K., Saftig, P., Khokha, R., Lundell, D., and Blobel, C. P. (2010) ADAM17 is regulated by a rapid and reversible mechanism that controls access to its catalytic site. *J. Cell Science* **123**, 3913-3922
  20. Maretzky, T., Evers, A., Zhou, W., Swendeman, S. L., Wong, P. M., Rafii, S., Reiss, K., and Blobel, C. P. (2011) Migration of growth factor-stimulated epithelial and endothelial cells depends on EGFR transactivation by ADAM17. *Nat Commun* **2**, 229
  21. Gschwind, A., Hart, S., Fischer, O. M., and Ullrich, A. (2003) TACE cleavage of proamphiregulin regulates GPCR-induced proliferation and motility of cancer cells. *Embo J.* **22**, 2411-2421
  22. Myers, T. J., Brennaman, L. H., Stevenson, M., Higashiyama, S., Russell, W. E., Lee, D. C., and Sunnarborg, S. W. (2009) Mitochondrial reactive oxygen species mediate GPCR-induced TACE/ADAM17-dependent transforming growth factor-alpha shedding. *Mol Biol Cell* **20**, 5236-5249
  23. Ohtsu, H., Dempsey, P. J., Frank, G. D., Brailoiu, E., Higuchi, S., Suzuki, H., Nakashima, H., Eguchi, K., and Eguchi, S. (2006) ADAM17 mediates epidermal growth factor receptor transactivation and vascular smooth muscle cell hypertrophy induced by angiotensin II. *Arterioscler Thromb Vasc Biol* **26**, e133-137
  24. Mcllwain, D. R., Lang, P. A., Maretzky, T., Hamada, K., Ohishi, K., Maney, S. K., Berger, T., Murthy, A., Duncan, G., Xu, H. C., Lang, K. S., Haussinger, D., Wakeham, A., Itie-Youten, A., Khokha, R., Ohashi, P. S., Blobel, C. P., and Mak, T. W. (2012) iRhom2 regulation of TACE controls TNF-mediated protection against *Listeria* and responses to LPS. *Science* **335**, 229-232
  25. Adrain, C., Zettl, M., Christova, Y., Taylor, N., and Freeman, M. (2012) Tumor necrosis factor signaling requires iRhom2 to promote trafficking and activation of TACE. *Science* **335**, 225-228

26. Siggs, O. M., Xiao, N., Wang, Y., Shi, H., Tomisato, W., Li, X., Xia, Y., and Beutler, B. (2012) iRhom2 is required for the secretion of mouse TNFalpha. *Blood* **119**, 5769-5771
27. Li, X., Maretzky, T., Weskamp, G., Monette, S., Qing, X., Issuree, P. D., Crawford, H. C., Mcllwain, D. R., Mak, T. W., Salmon, J. E., and Blobel, C. P. (2015) iRhoms 1 and 2 are essential upstream regulators of ADAM17-dependent EGFR signaling. *Proc Natl Acad Sci U S A* **112**, 6080-6085
28. Li, X., Maretzky, T., Perez-Aguilar, J. M., Monette, S., Weskamp, G., Le Gall, S., Beutler, B., Weinstein, H., and Blobel, C. P. (2017) Structural modeling defines transmembrane residues in ADAM17 that are crucial for Rhbdf2/ADAM17-dependent proteolysis. *J Cell Sci* **130**, 868-878
29. Maretzky, T., Mcllwain, D. R., Issuree, P. D., Li, X., Malapeira, J., Amin, S., Lang, P. A., Mak, T. W., and Blobel, C. P. (2013) iRhom2 controls the substrate selectivity of stimulated ADAM17-dependent ectodomain shedding. *Proc Natl Acad Sci U S A* **110**, 11433-11438
30. Grieve, A. G., Xu, H., Kunzel, U., Bambrough, P., Sieber, B., and Freeman, M. (2017) Phosphorylation of iRhom2 at the plasma membrane controls mammalian TACE-dependent inflammatory and growth factor signalling. *Elife* **6**
31. Cavadas, M., Oikonomidi, I., Gaspar, C. J., Burbridge, E., Badenes, M., Felix, I., Bolado, A., Hu, T., Bileck, A., Gerner, C., Domingos, P. M., von Kriegsheim, A., and Adrain, C. (2017) Phosphorylation of iRhom2 Controls Stimulated Proteolytic Shedding by the Metalloprotease ADAM17/TACE. *Cell Rep* **21**, 745-757
32. Oikonomidi, I., Burbridge, E., Cavadas, M., Sullivan, G., Collis, B., Naegele, H., Clancy, D., Brezinova, J., Hu, T., Bileck, A., Gerner, C., Bolado, A., von Kriegsheim, A., Martin, S. J., Steinberg, F., Strisovsky, K., and Adrain, C. (2018) iTAP, a novel iRhom interactor, controls TNF secretion by policing the stability of iRhom/TACE. *Elife* **7**
33. Kunzel, U., Grieve, A. G., Meng, Y., Sieber, B., Cowley, S. A., and Freeman, M. (2018) FRMD8 promotes inflammatory and growth factor signalling by stabilising the iRhom/ADAM17 sheddase complex. *Elife* **7**
34. Maney, S. K., Mcllwain, D. R., Polz, R., Pandyra, A. A., Sundaram, B., Wolff, D., Ohishi, K., Maretzky, T., Brooke, M. A., Evers, A., Vasudevan, A. A., Aghaeepour, N., Scheller, J., Munk, C., Haussinger, D., Mak, T. W., Nolan, G. P., Kelsell, D. P., Blobel, C. P., Lang, K. S., and Lang, P. A. (2015) Deletions in the cytoplasmic domain of iRhom1 and iRhom2 promote shedding of the TNF receptor by the protease ADAM17. *Sci Signal* **8**, ra109
35. Luo, W. W., Li, S., Li, C., Lian, H., Yang, Q., Zhong, B., and Shu, H. B. (2016) iRhom2 is essential for innate immunity to DNA viruses by mediating trafficking and stability of the adaptor STING. *Nat Immunol* **17**, 1057-1066
36. Adrain, C., Strisovsky, K., Zettl, M., Hu, L., Lemberg, M. K., and Freeman, M. (2011) Mammalian EGF receptor activation by the rhomboid protease RHBDL2. *EMBO Rep* **12**, 421-427
37. Schlöndorff, J., Becherer, J. D., and Blobel, C. P. (2000) Intracellular maturation and localization of the tumour necrosis factor alpha convertase (TACE). *Biochem. J.* **347 Pt 1**, 131-138

38. Roghani, M., Becherer, J. D., Moss, M. L., Atherton, R. E., Erdjument-Bromage, H., Arribas, J., Blackburn, R. K., Weskamp, G., Tempst, P., and Blobel, C. P. (1999) Metalloprotease-disintegrin MDC9: intracellular maturation and catalytic activity. *J. Biol. Chem.* **274**, 3531-3540
39. Lee, D. H., and Goldberg, A. L. (1998) Proteasome inhibitors: valuable new tools for cell biologists. *Trends Cell Biol* **8**, 397-403
40. Fiebiger, E., Hirsch, C., Vyas, J. M., Gordon, E., Ploegh, H. L., and Tortorella, D. (2004) Dissection of the dislocation pathway for type I membrane proteins with a new small molecule inhibitor, eeyarestatin. *Mol Biol Cell* **15**, 1635-1646
41. Mauvezin, C., and Neufeld, T. P. (2015) Bafilomycin A1 disrupts autophagic flux by inhibiting both V-ATPase-dependent acidification and Ca-P60A/SERCA-dependent autophagosome-lysosome fusion. *Autophagy* **11**, 1437-1438
42. Pasquier, B. (2016) Autophagy inhibitors. *Cell Mol Life Sci* **73**, 985-1001
43. Wang, Q., Li, L., and Ye, Y. (2008) Inhibition of p97-dependent protein degradation by Eeyarestatin I. *J Biol Chem* **283**, 7445-7454
44. Myeku, N., and Figueiredo-Pereira, M. E. (2011) Dynamics of the degradation of ubiquitinated proteins by proteasomes and autophagy: association with sequestosome 1/p62. *J Biol Chem* **286**, 22426-22440
45. Adrain, C., and Freeman, M. (2012) New lives for old: evolution of pseudoenzyme function illustrated by iRhoms. *Nat Rev Mol Cell Biol* **13**, 489-498
46. Wong, E., Maretzky, T., Peleg, Y., Blobel, C. P., and Sagi, I. (2015) The Functional Maturation of A Disintegrin and Metalloproteinase (ADAM) 9, 10, and 17 Requires Processing at a Newly Identified Proprotein Convertase (PC) Cleavage Site. *J Biol Chem* **290**, 12135-12146
47. Hosur, V., Johnson, K. R., Burzenski, L. M., Stearns, T. M., Maser, R. S., and Shultz, L. D. (2014) Rhd2 mutations increase its protein stability and drive EGFR hyperactivation through enhanced secretion of amphiregulin. *Proc Natl Acad Sci U S A* **111**, E2200-2209
48. Siggs, O. M., Grieve, A., Xu, H., Bambrough, P., Christova, Y., and Freeman, M. (2014) Genetic interaction implicates iRhom2 in the regulation of EGF receptor signalling in mice. *Biol Open* **3**, 1151-1157
49. Kohler, G., and Milstein, C. (1975) Continuous cultures of fused cells secreting antibody of predefined specificity. *Nature* **256**, 495-497
50. Weskamp, G., Krätzschmar, J. R., Reid, M., and Blobel, C. P. (1996) MDC9, a widely expressed cellular disintegrin containing cytoplasmic SH3 ligand domains. *J. Cell Biol.* **132**, 717-726
51. Maretzky, T., Yang, G., Ouerfelli, O., Overall, C. M., Worpenberg, S., Hassiepen, U., Eder, J., and Blobel, C. P. (2009) Characterization of the catalytic activity of the membrane-anchored metalloproteinase ADAM15 in cell-based assays. *Biochem J* **420**, 105-113
52. Dai, P., Wang, W., Yang, N., Serna-Tamayo, C., Ricca, J. M., Zamarin, D., Shuman, S., Merghoub, T., Wolchok, J. D., and Deng, L. (2017) Intratumoral delivery of inactivated modified vaccinia virus Ankara (iMVA) induces systemic antitumor immunity via STING and Batf3-dependent dendritic cells. *Sci Immunol* **2**
53. Sauer, J. D., Sotelo-Troha, K., von Moltke, J., Monroe, K. M., Rae, C. S., Brubaker, S. W., Hyodo, M., Hayakawa, Y., Woodward, J. J., Portnoy, D. A., and Vance, R. E.

- (2011) The N-ethyl-N-nitrosourea-induced Goldenticket mouse mutant reveals an essential function of Sting in the in vivo interferon response to *Listeria monocytogenes* and cyclic dinucleotides. *Infect Immun* **79**, 688-694
54. Sahin, U., Weskamp, G., Zheng, Y., Chesneau, V., Horiuchi, K., and Blobel, C. P. (2006) A sensitive method to monitor ectodomain shedding of ligands of the epidermal growth factor receptor. in *Epidermal Growth Factor: Methods and Protocols* (T.B. Patel, and Bertics, P. J. eds.), Humana Press Inc., Totowa, NJ. pp 99-113

**Footnotes:** Abbreviations: Rhbdf1/2, Rhomboid 5 Homolog 1/2; iRhom1/2, inactive Rhomboid like protein 1/2; ADAM17, a disintegrin and metalloprotease 17; TNF $\alpha$ , tumor necrosis factor  $\alpha$ ; ER, endoplasmic reticulum, TGN, trans Golgi network; IL-6, interleukin 6; TMD, transmembrane domain; LPS, lipopolysaccharide; BMDM, bone marrow derived macrophages; EndoH, endoglycosidase H; PNGaseF, N-Glycosidase F; EGFR, epidermal growth factor receptor, STING, stimulator of interferon genes.

**Figure 1**

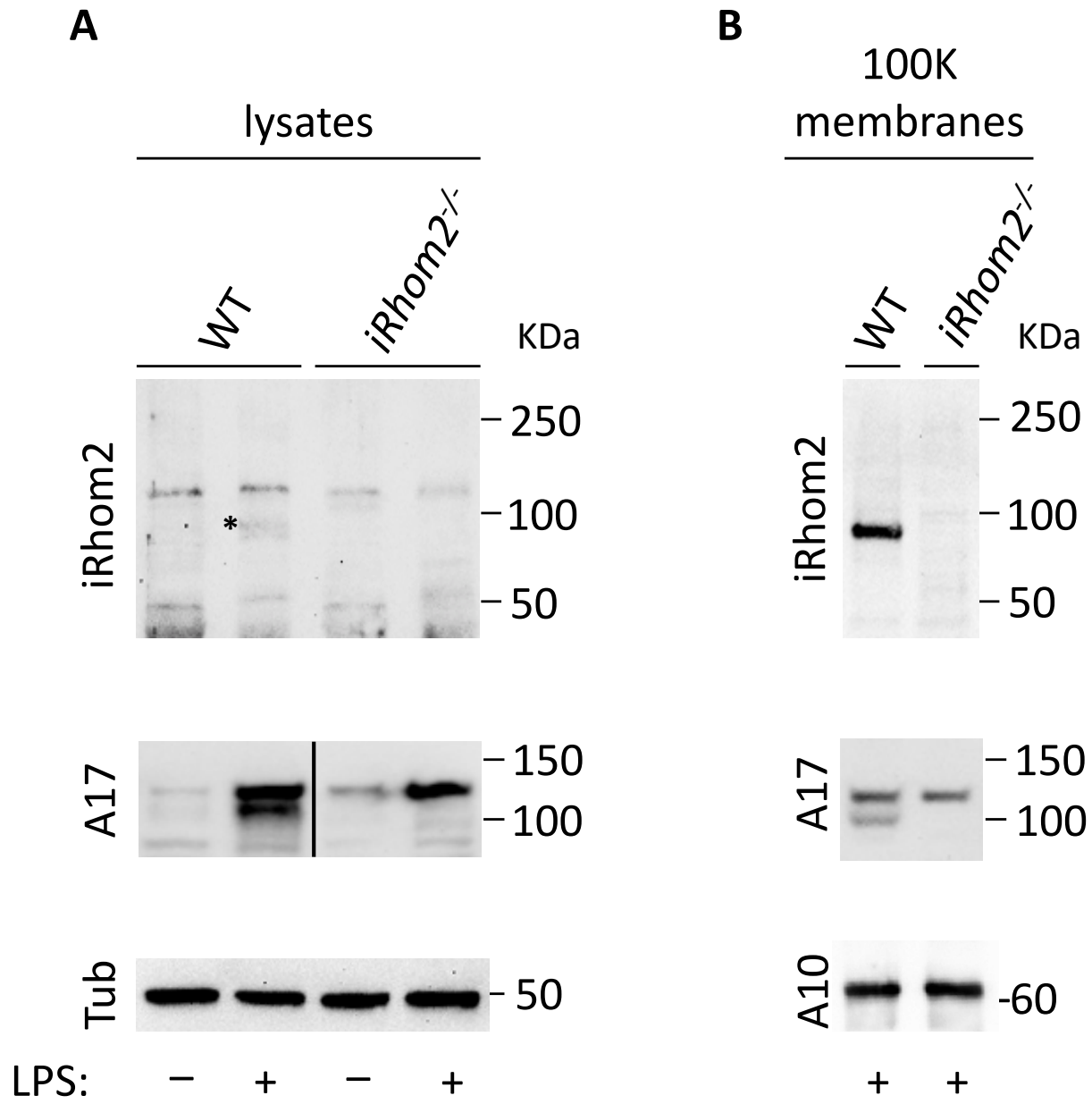


Figure 2

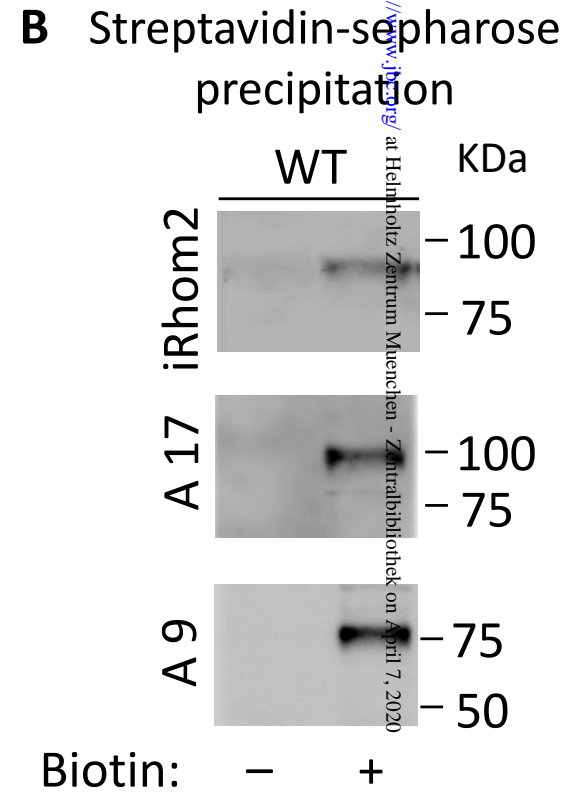
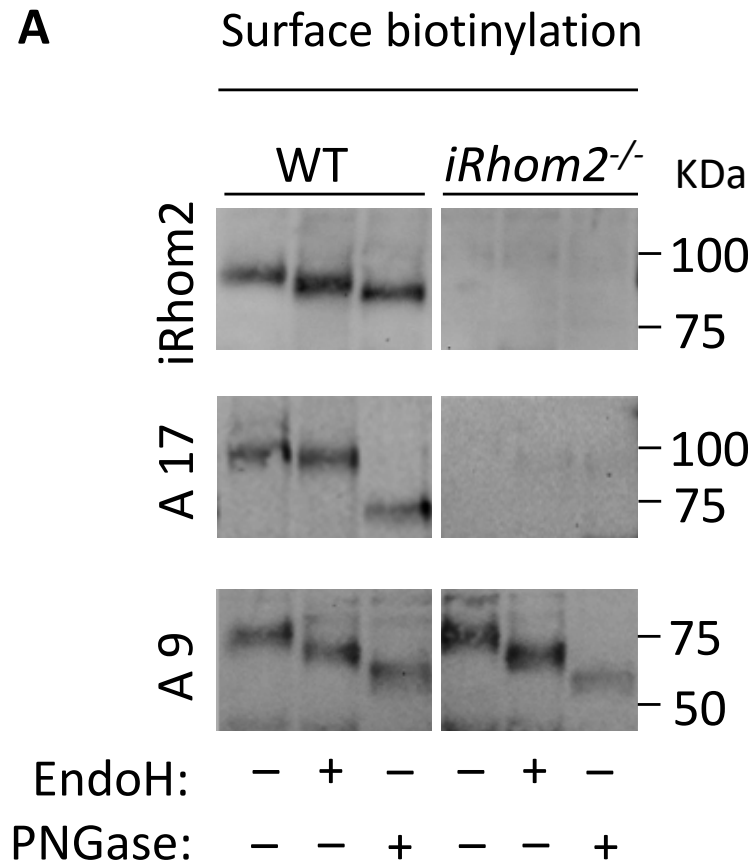


Figure 3

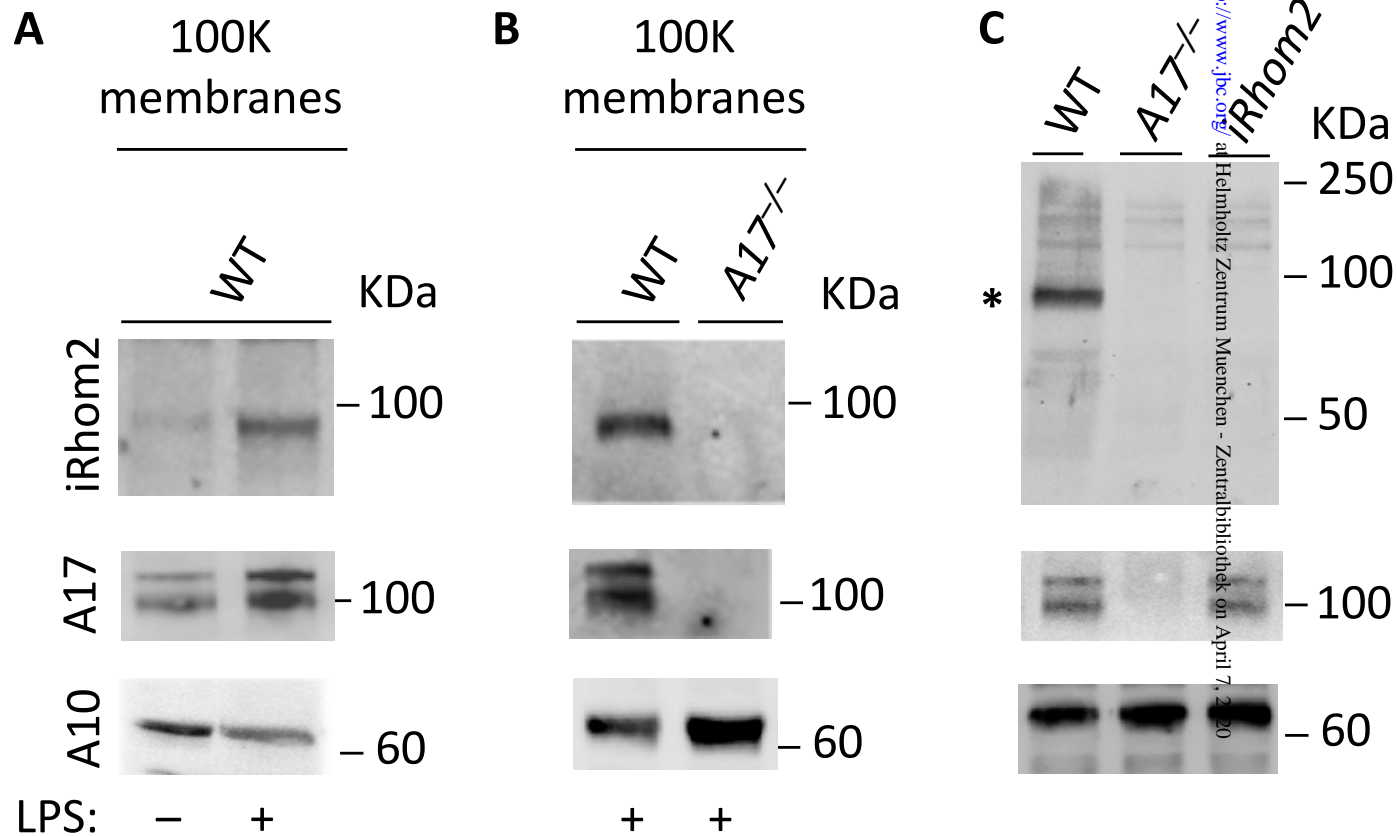
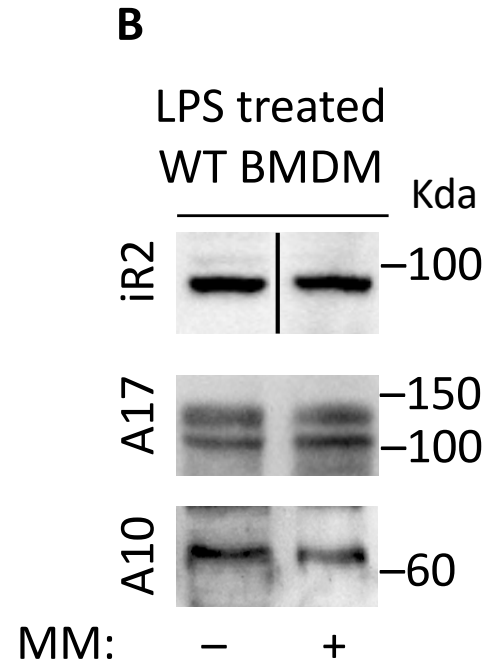
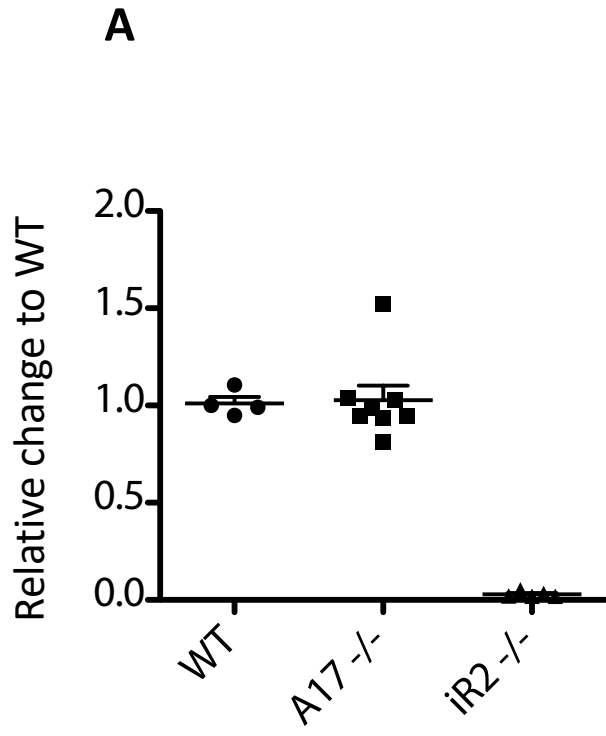
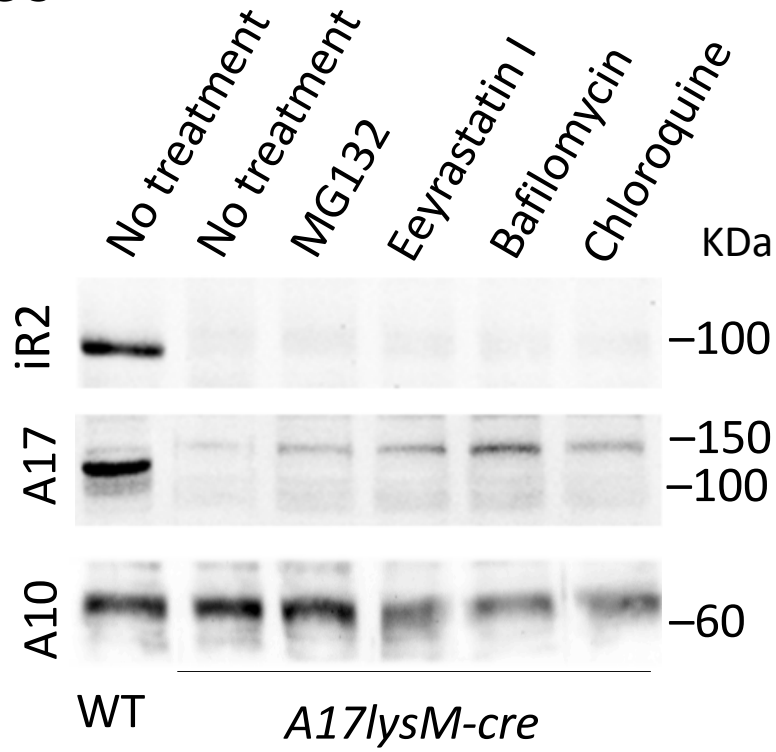


Figure 4

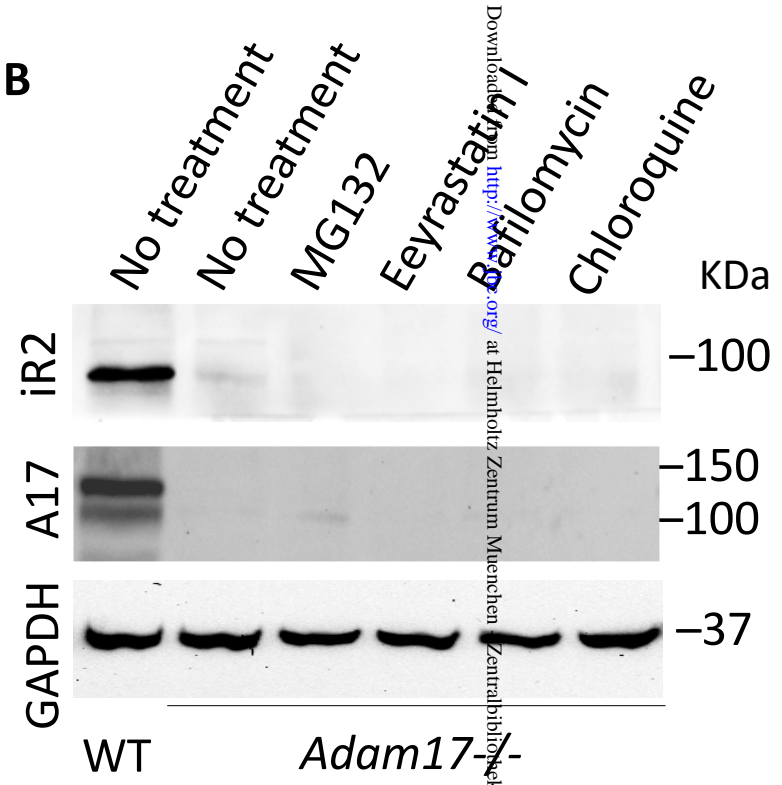


**Figure 5**

**A**

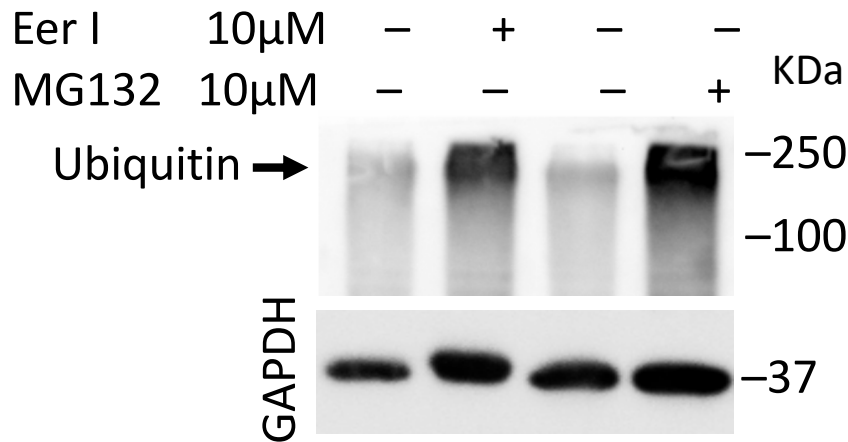


**B**



Downloaded from <http://www.jbc.org/> at Helmholtz Zentrum Muenchen - Zentralbibliothek on April 7, 2020

**C**



**D**

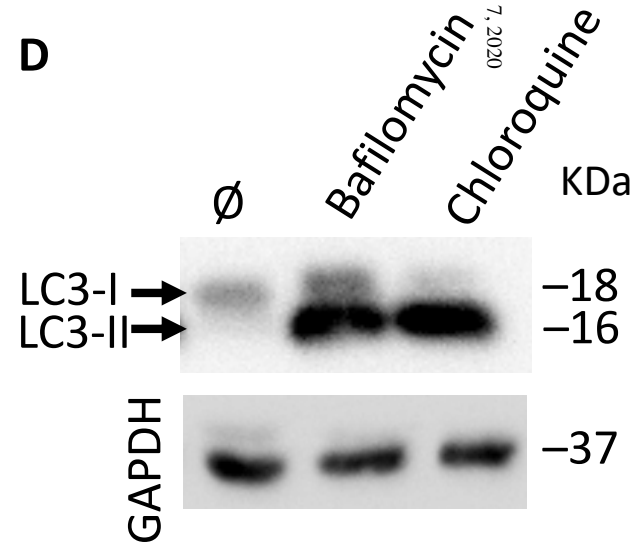


Figure 6

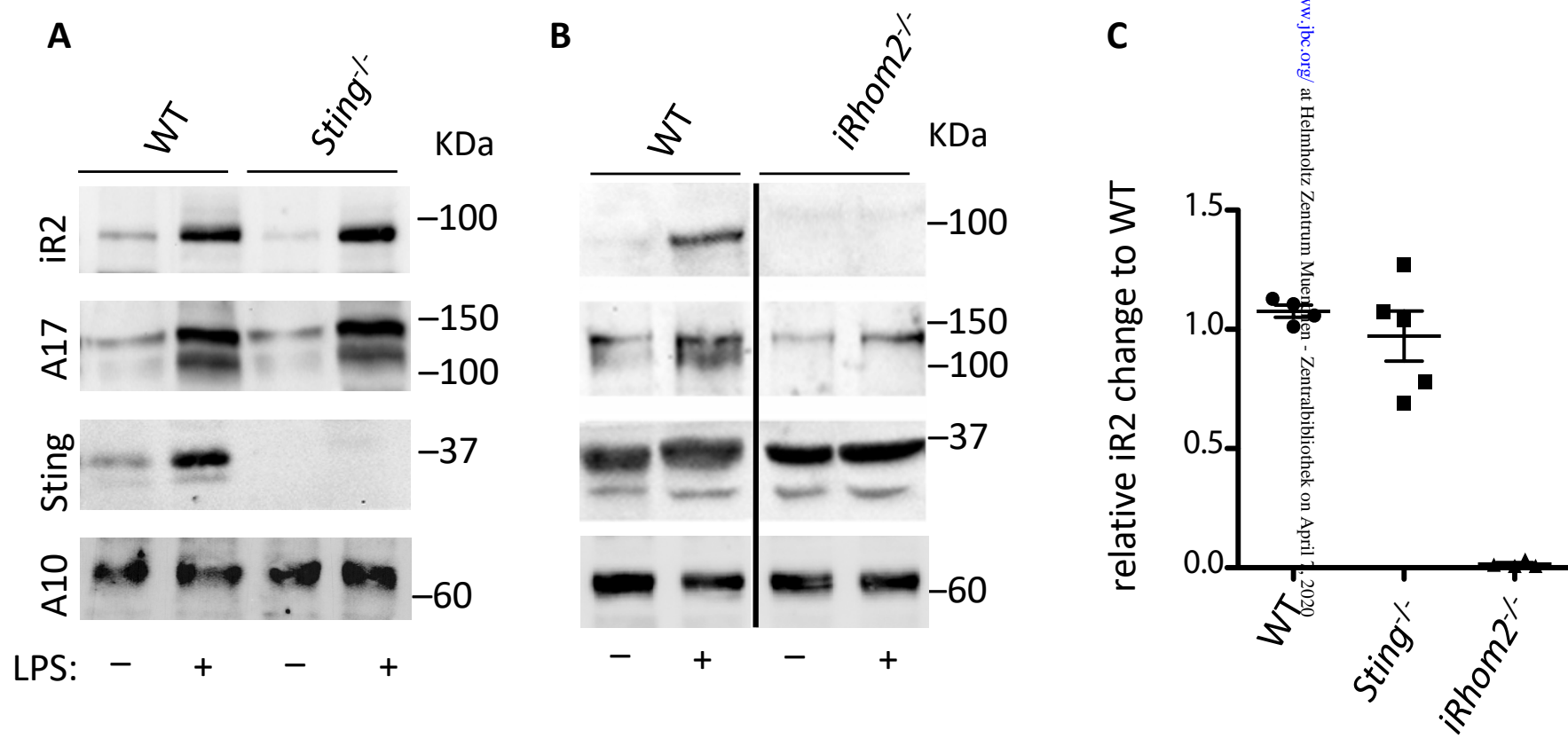
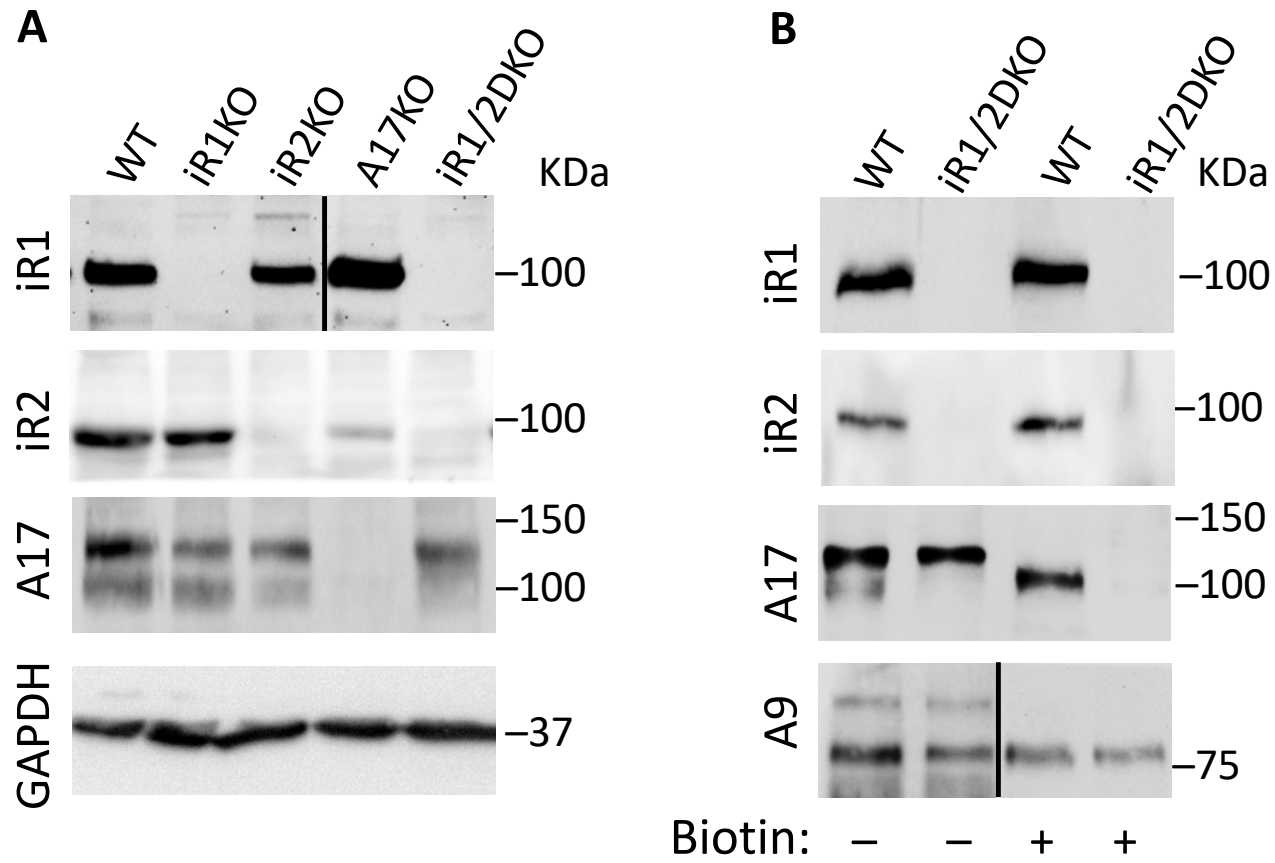


Figure 7



**ADAM17 stabilizes its interacting partner inactive Rhomboid 2 (iRhom2) but not inactive Rhomboid 1 (iRhom1)**

Gisela Weskamp, Johanna Tüshaus, Daniel Li, Regina Feederle, Thorsten Maretzky, Steven Swendeman, Erik Falck-Pedersen, David R. McIlwain, Tak W. Mak, Jane E Salmon, Stefan F Lichtenthaler and Carl P. Blobel

*J. Biol. Chem.* published online February 14, 2020

---

Access the most updated version of this article at doi: [10.1074/jbc.RA119.011136](https://doi.org/10.1074/jbc.RA119.011136)

Alerts:

- [When this article is cited](#)
- [When a correction for this article is posted](#)

[Click here](#) to choose from all of JBC's e-mail alerts